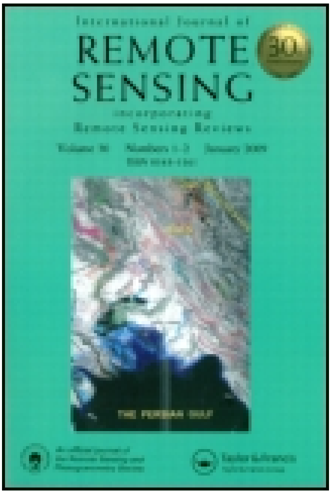

International Journal of Remote Sensing
Publication details, including instructions for authors and subscription information:
http://www.tandfonline.com/loi/tres20

Satellite-based mapping of Canadian boreal forest fires: Evaluation and comparison of algorithms

Z. Li [a], S. Nadon [b], J. Cihlar [a] & B. Stocks [c]
[a] Canada Centre for Remote Sensing, 588 Booth, Ottawa, Ontario, Canada, K1A OY7
[b] Environment Canada, Ottawa, Ontario, Canada, K1A OH3
[c] Canadian Forest Service, Sault Ste Marie, Ontario, Canada
Published online: 25 Nov 2010.

INT. J. REMOTE SENSING, 2000, VOL. 21, NO. 16, 3071–3082

Satellite-based mapping of Canadian boreal forest fires: evaluation and comparison of algorithms

Z. LI†*, S. NADON‡, J. CIHLAR† and B. STOCKS§

†Canada Centre for Remote Sensing, 588 Booth, Ottawa, Ontario, Canada, K1A OY7
‡Environment Canada, Ottawa, Ontario, Canada, K1A OH3
§Canadian Forest Service, Sault Ste Marie, Ontario, Canada

(*Received 27 September 1998; in final form 4 June 1999*)

Abstract. This paper evaluates annual fire maps that were produced from NOAA-14/AVHRR imagery using an algorithm described in a companion paper (Li *et al*., *International Journal of Remote Sensing*, **21**, 3057–3069, 2000 (this issue)). Burned area masks covering the Canadian boreal forest were created by compositing the daily maps of fire hot spots over the summer and by examining Normalized Difference Vegetation Index (NDVI) changes after burning. Both masks were compared with fire polygons derived by Canadian fire agencies through aerial surveillance. It was found that the majority of fire events were captured by the satellite-based techniques, but burnt area was generally underestimated. The burn boundary formed by the fire pixels detected by satellite were in good agreement with the polygons boundaries within which, however, there were some fires missed by the satellite. The presence of clouds and low sampling frequency of satellite observation are the two major causes for the underestimation. While this problem is alleviated by taking advantage of NDVI changes, a simple combination of a hot spot technique with a NDVI method is not an ideal solution due to the introduction of new sources of uncertainty.

In addition, the performance of the algorithm used in the International Geosphere–Biosphere Programme (IGBP) Data and Information System (IGBP-DIS) for global fire detection was evaluated by comparing its results with ours and with the fire agency reports. It was found that the IGBP-DIS algorithm is capable of detecting the majority of fires over the boreal forest, but also includes many false fires over old burned scars created by fires taking place in previous years. A step-by-step comparison between the two algorithms revealed the causes of the problem and recommendations are made to rectify them.

1. Introduction

Forest fires can have major environmental and economic impact. In Canada alone, about 9000 fires, on average, burn every year consuming an average of about 2.5 Mha of forests (Stocks *et al.* 1996, Li *et al.* 2000). Such average statistics are, however, of limited significance, as the area burned in boreal forests shows a tremendous inter-annual variation. For example, the total burnt area across Canada can differ by a factor of more than 12 within a couple of years, e.g. 5.1 Mha in 1995 and

*Corresponding author; e-mail: li@ccrs.nrcan.gc.ca

International Journal of Remote Sensing
ISSN 0143-1161 print/ISSN 1366-5901 online © 2000 Government of Canada
http://www.tandf.co.uk/journals

0.4 Mha in 1997 according to satellite-based estimation (Li *et al.* 2000). Much of the area burned was observed in remote regions of Canada.

Information on wild fires can be collected by a variety of means. Among those, the most frequently used are traditional ground-based *in situ* observation, air-borne human and photographic surveillance, and space-borne remote sensing. The quality, density and frequency of ground-based and air-borne fire observations vary considerably from one country or region to another. Only satellites offer the potential to acquire global uniform fire information on a repetitive basis. However, like many optical remote sensing techniques, satellite fire detection algorithms have some disadvantages.

The largest problem is cloud cover below which no fires can be detected, an inherent limitation for most optical remote sensing applications. A lack of temporal sampling and a limited range of radiometric sensitivity are the major shortcomings of the Advanced Very High Resolution Radiometer (AVHRR), which has been most widely used for fire detection (Justice *et al.* 1996). The quality of fire data inferred from satellites thus warrants thorough assessment. Unfortunately, only a handful of studies using satellite sensor data to detect and map fires include validation exercises due to limited ground data on actual fires (e.g. Setzer *et al.* 1994, Li *et al.* 1997).

This study presents an in-depth evaluation of a fire database derived from daily AVHRR satellite images (Li *et al.* 2000). The database was created by applying a fire-detection algorithm that was developed at the Canada Centre for Remote Sensing (CCRS) which is hereafter referred to as the CCRS fire-detection algorithm (CFDA). Section 2 compares yearly accumulated areas of satellite-detected fire pixels to annual burnt area as reported by Canadian fire management agencies. The accumulated areas of ongoing fires are also compared with the areas of fire scars detected using the Normalized Difference Vegetation Index (NDVI) in §3.

In addition, §4 of this paper presents a comparison of the CFDA to a global fire-detection algorithm developed and used in the International Geosphere–Biosphere Programme Data and Information System (IGBP-DIS) (Justice *et al.* 1996, Malingreau and Gregoire 1996, IGBP 1997). The algorithm was intended to generate a global *coherent* and *consistent* biomass burning dataset. The major difference between the CFDA and the IGBP algorithm is that the CFDA is a traditional threshold algorithm using fixed values while the IGBP algorithm is a contextual algorithm that relies on local background information to dynamically set thresholds. As a result, the IGBP algorithm was designed to be self-adaptive and consistent over large areas under different environmental conditions (Flasse and Ceccato 1996). Careful evaluation of this algorithm in different parts of the world is essential to achieve the goal of the IGBP fire project. The objective of §4 is to test if the IGBP algorithm is self-adaptive enough to be effective over Canadian boreal forests.

2. Evaluation of fire hot spots

Canada routinely gathers and maintains rather detailed and complete records of forest fires, which enables a comprehensive evaluation of satellite detection results, thanks to provincial and territorial fire management agencies. Fire polygon data were acquired by means of airborne infrared mapping. Data from all agencies were compiled to determine the total area burned in Canada. No standard data format exists among the provinces and territories and the data quality and availability may vary from one province/territory to another. The Canadian Forest Service (CFS) established a National Forestry Database Program to gather, process and standardize fire information in digital format and distribute them in a geographic information system (GIS). Such data in two regions of Northwest Territories and Saskatchewan in 1995 were employed in this investigation. Each of the two regions contains 1375×1200 1 km pixels.

Figure 1 presents comparisons of these data to the annual composites of fire pixels detected by satellite over the two regions. The blue polygons outline the boundaries of burnt area reported by fire agencies while red dots are locations of active fire pixels detected during the entire fire season. In Saskatchewan, 47 major fire events were reported by fire agencies and all of them were detected by the CFDA.

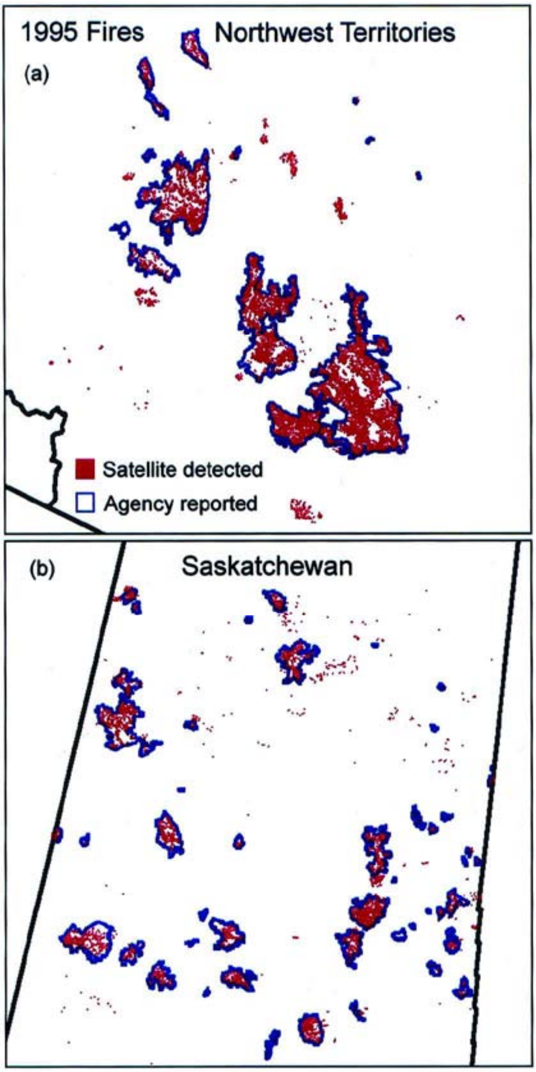

Figure 1. Comparison of the annual composite of fire spots with data obtained by fire agencies for two regions in Canada in 1995. The blue polygons outline the boundaries of burnt area reported by fire agencies using conventional means of monitoring while red dots are locations of active fire pixels observed by satellite during an entire fire season.

In the Northwest Territories, there are 24 large fires reported by fire agencies, six of which were missed by satellite. However, the missed fires covered small areas on the order of 1000 ha. Combining data from the two regions, we calculated that 7.3% of the pixels showing fire activity fall outside the burnt area boundaries reported by fire agencies. We visually inspected satellite images for all the cases in which satellite detects fire activities which were not reported by fire agencies. It was determined that 20% of these pixels have smoke associated with them. Most of the large fire clusters detected by satellite show some smoke phenomena. These seemingly real fires were not reported by fire agencies. Only 5.8% of the pixels that are detected by satellite as fires are not certain. Their sizes are very small (smaller than 300 ha). Therefore, the probability that pixels detected by satellites as fires are true fires (> 300 ha) is as high as 94%.

Figure 2 is a histogram showing the frequency of pixels detected as fires inside the fire polygons. This figure shows that about 60% of the fire pixels were detected only once and 26% twice. This suggests that the success of fire monitoring from space depends very much on the frequency of satellite overpass, the speed of fire spreading and the amount of cloud cover. These factors partially explain why the yearly hot spot composite is patchy rather than continuous. On the other hand, however, the area inside the polygons reported by fire agencies is not necessarily completely burned, as is shown in the next section.

3. Comparison against satellite-detected fire scars

The potential of the CFDA in mapping burnt area is also evaluated by comparing areas of fire hot spots detected from individual AVHRR images with fire scars detected from AVHRR clear-sky composites. Several studies have shown that fire scars may be visible from the difference in vegetation indices before and after burning in boreal and temperate forests (Cahoon *et al.* 1992, Kasischke *et al.* 1993, Kasischke and French 1995, Li *et al.* 1997). Here, we examine changes in NDVI between two consecutive years. Clear-sky composite data of maximal NDVI over 10-day periods are available across Canada since 1993 following a series of corrections (Cihlar *et al.* 1997). Twenty 10-day composites from 20 April to 10 November were processed every year except for 1994 when the data for the last five composites were unavailable.

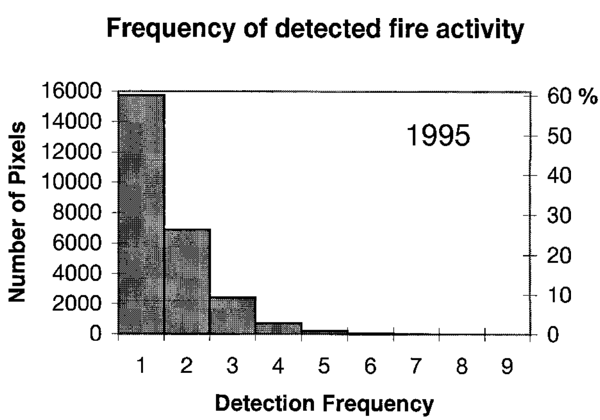

Figure 2. Histogram of the frequency of satellite-detected fire pixels inside the polygons shown in figure 1.

Under normal conditions, NDVI exhibits a clear seasonal cycle. It increases gradually in spring, reaches a peak value in August, and then declines quickly in autumn. Such a seasonal cycle may shift earlier or later depending on climate.

Following a fire event, NDVI has a sharp drop. The method used here is intended to detect all new fire scars in a particular year. In order to do so, two pairs of NDVI images were employed, one in spring and another in autumn. Note that the years of the two consecutive periods are different. For example, to determine the 1995 fire scars as shown here, the spring pair comes from 1995 and 1996 images, while the autumn pair consists of 1994 and 1995 images. Comparing NDVI images from the same period of the year, as opposed to comparing spring and autumn images from the same year, can overcome the problem associated with the annual NDVI cycle. Comparisons of NDVI for two periods reduce the noise introduced by the inter-annual variation of NDVI. The spring and autumn periods were chosen to be 21–31 May and 11–20 September, respectively. Contained within the two periods is the bulk of a fire season without snow cover in the region of interest. Snow cover over forest diminishes the NDVI drastically.

The difference in NDVI was computed pixel by pixel for each pair of the images. A threshold was then used to identify pixels with scar signature. After some tests, a relative NDVI change of 9% was found to separate most fire scars from the background. Pixels that showed a relative NDVI drop greater than 9% in both pairs of images were marked as fire scar pixels.

Figure 3 presents a comparison of the results obtained with the CFDA and the scar detection method in the same two regions as shown earlier. Three colours are used to denote fire pixels detected by the CFDA alone (red), the scar method alone (green) and by both methods (yellow), in comparison with the blue fire boundaries reported by fire agencies. It is evident that the fire scars determined from NDVI agree well with the areas of the polygons. Fire pixels determined by the CFDA (red and yellow) occupy about 60% of the area inside the blue outlines. The fire scars (green and yellow) derived from NDVI cover about 63% of the total area of the polygons. About half of the total fire pixels are identified by both methods. These overlapped pixels have the highest probability of being true fires. On the contrary, pixels inside the polygons that are not marked by either algorithm are more likely to be unburned patches. They occupy 19% of the total areas of the polygons, with 1.4% identified as water bodies.

Limitations in the detection methods caused a significant portion of the burnt area to be detected by only one method. For the CFDA, cloud cover and insufficient temporal sampling were dominant factors. For the NDVI scar detection method, sub-grid burning and burns of little damage (most likely surface fires) were hard to detect. In addition, a change in NDVI may be caused by something other than a fire, such as drought, tree diseases, insects, etc. The most prominent problem in the NDVI approach is probably associated with cloud contamination, which can reduce NDVI value considerably. Although great care was exercised to remove cloud contaminated pixels in generating clear composite data (Cihlar *et al.* 1997), there is no assurance that all pixels are cloud-free, in particular for residual clouds and persistent clouds. These limitations lead to a considerable number of scattered false fire pixels that are evident in figure 3. Therefore, a simple combination of the two methods may not be ideal in mapping burned area, as both real and false fires accumulate concurrently. As such, a new synergistic method based on hot spot and NDVI has been developed that takes advantage of the strengths of each method, while at the same time avoiding their weakness (Fraser *et al.* 1999).

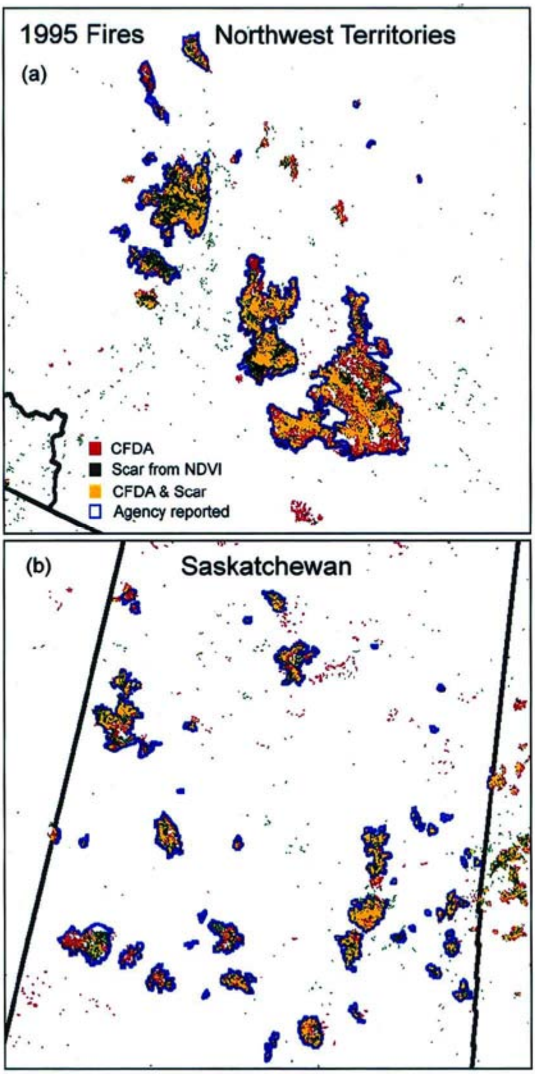

Figure 3. Comparison of the annual composite of fire spots for 1995 with fire scars detected using NDVI in two regions of Canada. Red dots represent fire pixels detected by single-day AVHRR algorithm only, while green dots are fire pixels identified using NDVI only. Yellow represents fire pixels that are detected by both techniques.

4. Comparison with IGBP algorithm

The DIS group of the International Geosphere–Biosphere Program (IGBP-DIS) developed an algorithm for global fire moritoring using AVHRR data. To date, this algorithm has been employed to process NOAA-11 data over most parts of the tropical regions for a period of 21 months between April 1992 and December 1993 (IGBP-DIS WWW site: http://www.mtv.sai.irc.it/projects/fire/gfp/home.html).

The IGBP algorithm was designed to generate a global, uniform fire database in order to provide better information on the spatial and temporal distribution of fire at a global scale. The CFDA algorithm was designed for specific use in boreal forests.

For the sake of understanding and comparing the performance of the two algorithms, the IGBP algorithm is described first with reference to CFDA.

4.1. *Comparative description of the IGBP algorithm*

In an attempt to avoid the need for adjusting the algorithm over different regions or ecosystems, the method employed by IGBP is a contextual approach (Flasse and Ceccato 1996, Justice *et al.* 1996, IGBP 1997). The decision to designate a pixel as a fire or not is based on comparison of its radiometric signature with those from surrounding pixels. The first step of the method applies absolute thresholds to mark all pixels that have:

$$T_3 > 311\,\mathrm{K} \text{ and } T_3 - T_4 > 8\,\mathrm{K} \tag{1}$$

as potential fires, where T_3 and T_4 are the brightness temperatures in AVHRR channel 3 and 4. The second step consists of contextual tests whereby T_3 and $T_3 - T_4$ for potential fires are compared with the corresponding average values calculated from the pixels surrounding the potential fire pixels under study. Pixels that are potential fires, water or clouds are excluded from the computation. The remaining pixels are simply referred to as normal background pixels. Water pixels are identified using a land-water mask while cloud pixels are identified following a threshold test. The contextual tests confirm a potential fire pixel as being true if it passes the following criteria tests[1]:

$$[T_3 - T_4] > \max\,\{T_{34\mathrm{bg}} + 2\,\sigma_{34\mathrm{bg}}, 8\,\mathrm{K}\} \tag{2}$$

and

$$T_3 > T_{3\mathrm{bg}} + 2\,\sigma_{3\mathrm{bg}} + 3\,\mathrm{K} \tag{3}$$

where $T_{3\mathrm{bg}}$ is the mean background brightness temperature in channel 3; $\sigma_{3\mathrm{bg}}$ the standard deviation of background T_3; $T_{34\mathrm{bg}}$ the mean value of background $[T_3 - T_4]$; and $\sigma_{34\mathrm{bg}}$ the standard deviation of background $[T_3 - T_4]$. The background pixels used to compute these statistical thresholds are from a window centred at the potential fire pixel under testing. The window has an initial dimension of 3×3 pixels and is allowed to grow gradually up to 15×15 pixels, or until at least 25% of the pixels inside the window qualify as normal background pixels. If the window reaches the largest size and less than 25% of the pixels inside are deemed as background, the potential fire pixel under study is not confirmed.

It follows that the thresholds are dynamic variables, in contrast to the fixed values used in CFDA. To gain a sense of their magnitude in the boreal forest application, the values obtained during the execution of the IGPB algorithm over a scene of 1200×1200 pixels on 24 June 1995 were saved and analysed. Table 1 delineates the overall statistics of these parameters for the 48 214 pixels identified as potential fires.

To put these values in context, they are compared with those used in the CFDA, in table 2. Table 2 also provides a complete comparison of all the tests used in the two algorithms. The order of the tests as listed is not necessarily the same as that used in the code. Similar tests have been grouped together on the same line of the

[1] There appears to be an error in the original document (IGBP 1997) describing the IGBP method in which 3 K was used instead of 8 K, which contradicts equation (1). If a pixel is declared as a potential fire by (1), $T_3 - T_4$ must be larger than 8 K.

Table 1. The statistics of the IGBP contextual thresholds obtained over a boreal forest region.

Parameter	Mean value (K)	SD (K)
T_{34bg}	7.9	2.9
σ_{34bg}	1.6	1.8
T_{3bg}	310	3
σ_{3bg}	2.1	1.3
$T_{34bg}+2\sigma_{34bg}$	11	6
$T_{3bg}+2\sigma_{3bg}+3$	317	3

Table 2. A comparison of CFDA and IGBP algorithms.

CFDA NOAA-14	IGBP algorithm
$T_3 > 315$ K	potential fire test: $T_3 > 311$ K contextual test: $T_3 > 317$ K (mean)
$T_3 - T_4 < 14$ K	potential fire test: $T_3 - T_4 > 8$ K contextual test: $T_3 - T_4 > 11$ (mean)
$R_2 < 0.22$	$R_2 < 0.20$
eliminate cropland, grassland and water	eliminate water
$T_4 - T_5 < 4.1$ K and $T_3 - T_4 \geq 19$ K	–
–	sun-glint: $\lvert R_1 - R_2 \rvert \geq 0.02$
$T_4 > 260$ K	cloud: $T_5 \geq 265$ K
–	cloud: $R_1 + R_2 \leq 1.20$
–	cloud: $R_1 + R_2 \leq 0.8$ and $T_5 \geq 285$ K
eliminate single pixels	–

table. The listed contextual values are averages and the actual values used in the test vary from pixel to pixel. The range of variation is indicated by the standard deviations given in table 1.

The similarities and discrepancies between the two algorithms are evident from table 2, which helps understand the differences between the results obatined by the two fire-detection algorithms. Some key tests are common but may be in slightly different forms. The IGBP algorithm has more tests to eliminate cloud pixels. The IGBP sun-glint test was evaluated and was found to be inefficient for the current application. As a result of the contextual tests, execution of the IGBP algorithm is much more time-consuming than for the CFDA (10 times slower). This poses a concern for real-time fire detection, for which the CFDA is designed.

4.2. *Performance of the IGBP algorithm*

Figure 4 presents the results of fire detection using the IGBP algorithm for the 1995 fire season over the same two regions as shown in figure 1. The burnt areas from fire agencies again are depicted by the blue polygons. Fire pixels identified by the algorithm cover 48% of the area inside the fire polygons, compared with 60% for the CFDA. On the other hand, many pixels outside of the boundaries of the reported fires are marked as fires by the IGBP algorithm. With reference to figure 1, the proportion of false fires is considerably higher with the IGBP algorithm than with the CFDA. Figure 5 shows fire pixels detected by CFDA for both 1995 and 1994. A comparison between figures 4 and 5 indicates that the majority of the fire pixels outside of the polygons identified by IGBP algorithm are actually scars from

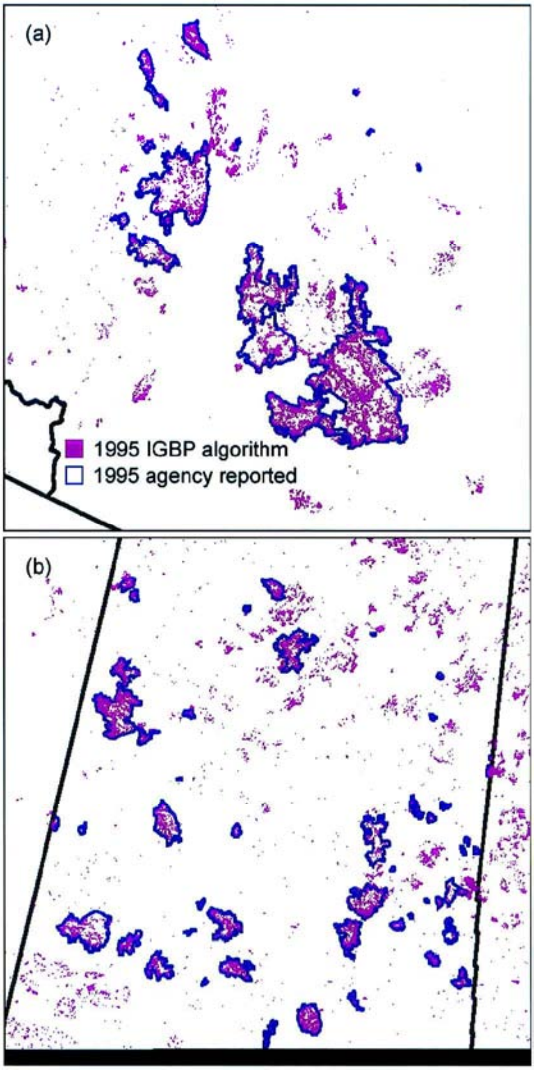

Figure 4. Same as figure 1 but using the IGBP fire-detection algorithm.

1994 fires. All major burns shown in figure 5 for 1994 were verified against ground data from fire agencies.

The reason that the IGBP algorithm misidentifies old fire scars as active fires appears to be that the thresholds for potential fire tests are set too low, which tends to confuse radiometric signals from fresh fire scars with on-going fires. Fresh scars have very low albedos and thus heat up more than forest, leading to a high brightness temperature. As a result, the test of T_3 for potential fires can be readily passed. The second test based on $T_3 - T_4$ is presumably insufficient to eliminate such a warm background. Since the statistics calculated for background pixels do not include potential fire pixels, many pixels surrounding the potential fire under examination are disqualified. The algorithm continues searching for colder background pixels.

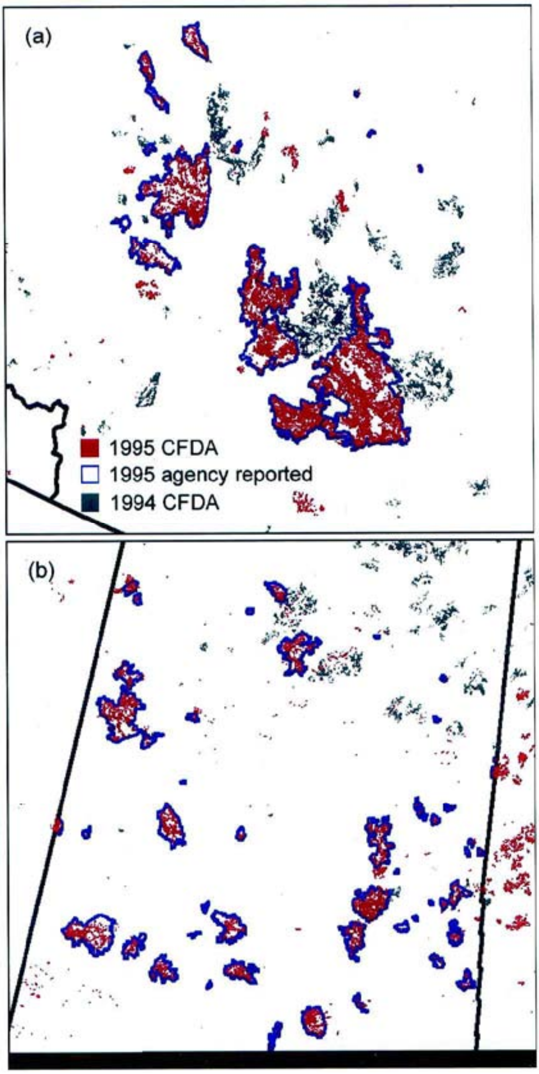

Figure 5. The distribution of fire pixels detected with the CFDA algorithm in 1995 (red dots) and in 1994 (grey dots).

At the end, the values of T_{3bg} and T_{34bg} obtained are lower than the actual background values, which favours the confirmation of these potential fire pixels by the contextual tests.

These results suggest that the IGBP algorithm is not self-adaptive enough to be used universally and blindly. After all, the IGBP algorithm relies on many fixed thresholds. Adjustments to these thresholds may be necessary. In this case, increasing the thresholds of T_3 and $T_3 - T_4$ would remedy the problem.

5. Conclusion

In this paper we evaluated the peformance of an algorithm developed to detect fires in the Canadian boreal forest based on NOAA AVHRR data. The evaluation used satellite sensor data and ground observations over parts of western Canada in 1995. The areas and locations of fires detected with a conventional method and from AVHRR satellite data (both individual daily images and 10-day clear composites) were compared. In addition, the satellite fire-detection algorithm that we developed (CFDA) and that designed for use by IGBP were compared. The findings of the study are summarized as follows.

- In comparison to the fires reported by Canadian fire agencies and those indicated by smoke plumes, the likelihood that a pixel was correctly identified by the CFDA as fire is as high as 94%.
- The majority of fire events are captured by satellite, but the area of burning given by an ensemble of fire pixels may be underestimated considerably (~ 35% on average) by satellite due to cloud cover and low frequency of satellite overpass.
- The combination of active fire detection and fire scar identification may considerably reduce the area of missed fires, but also concurrently increase the number of false fires.
- Relative to CFDA, the IGBP fire-detection algorithm developed for global applications suffers larger commission and omission errors when applied to boreal forest. It tends to mark some of the burned scars from previous year as active fires. Re-tuning of certain thresholds would be required to achieve high accuracy.

The study suggests that fire detection in boreal forests using AVHRR data is a viable strategy for obtaining timely and consistent fire information with acceptable accuracy. The major limitations of this data source are spatial resolution and clouds, which interfere with obtaining local detail and high temporal frequency, respectively. Future satellite sensors such as MODIS will reduce the former deficiency, while the latter requires new techniques such as the synergic combination of hot spots and NDVI differencing (Fraser *et al.* 1999). At any rate, the study demonstrates that satellite sensor data can serve as an important tool for acquiring timely and moderately accurate information on boreal forest fires for strategic and management applications.

Acknowledgements

The authors are grateful to John Mason, Sun Hua, Norm Mair and Bruno Croft for providing us with ground fire data, and Robert Fraser for comments.

References

Cahoon, D. R., Jr, Stocks, B. J., Levine, J. S., Cofer, W. R., III, and Chung, C. C., 1992, Evaluation of a technique for satellite-derived area estimation of forest fires. *Journal of Geophysical Research*, **97**, 3805–3814.

Cihlar, J., Chen, J., and Li, Z., 1997, Seasonal AVHRR multichannel data sets and products for studies of surface–atmosphere interactions. *Journal of Geophysical Research*, **102**, 29 625–29 640.

Flasse, S. P., and Ceccato, P. S., 1996, A contextual algorithm for AVHRR fire detection. *International Journal of Remote Sensing*, **17**, 419–424.

Fraser, R., Li, Z., and Cihlar, J., 1999, A new technique for mapping burns: hot spot and NDVI differencing synergy (HANDS). *Remote Sensing of Environment*, in press.

IGBP, 1997, Definition and implementation of a global fire product derived from AVHRR data. IGBP-DIS Working Paper no. 17.

Justice, C. O., Kendall, J. D., Dowty, P. R., and Scholes, R. J., 1996, Satellite remote sensing of fires during the SAFARI campaign using NOAA advanced very high resolution radiometer data. *Journal of Geophysical Research*, **101**, 23 851–23 863.

Kasischke, E. S., and French, N. H. F., 1995, Locating and estimating the areal extent of windfires in Alaskan boreal forests using multiple-season AVHRR NDVI composite data. *Remote Sensing of Environment*, **51**, 263–275.

Kasischke, E. S., French, N. H. F., Harrell, P., Christensen, N. L., Jr, Ustin, S. L., and Barry, D., 1993, Monitoring of wildfires in boreal forests using large area AVHRR NDVI composite image data. *Remote Sensing of Environment*, **45**, 61–71.

Li, Z., Cilar, J., Moreau, L., Huang, F., and Lee, B., 1997, Monitoring fire activities in the boreal ecosystem. *Journal of Geophysical Research*, **102**, 29 611–29 624.

Li, Z., Nadon, S., and Cihlar, J., 2000, Satellite-based detection of Canadian boreal forest fires: development and application of the algorithm. *International Journal of Remote Sensing*, **21**, 3057–3069.

Malingreau, J. P., and Gregoire, J.-M., 1996, Developing a global vegetation fire monitoring system for global change studies: a framework. In *Biomass Burning and Global Change*, edited by J. S. Levine (Cambridge, MA: The MIT Press), pp. 14–24.

Setzer, A. W., Pereira, A. C., and Pereira, M. C., 1994, Satellite studies of biomass burning in Amazonia: some practical aspects. *Remote Sensing Reviews*, **10**, 91–103.

Stocks, B. J., Lee, B. S., and Martell, D. C., 1996, Some potential carbon budget implications of fire management in the boreal forest. In *Forest Ecosystems, Forest Management and the Global Carbon Cycle*, edited by M. J. Apps and D. T. Price, NATO ASI Series, Sub-series 1, vol. 40, *Global Environmental Change* (Berlin: Springer), pp. 89–96.